DTU Library

Modeling the mechanical deformation of nickel foils for nanoimprint lithography on double-curved surfaces

Sonne, Mads Rostgaard; Cech, Jiri; Hattel, Jesper Henri; Taboryski, Rafael J.

[Link back to DTU Orbit](#)

Modelling the mechanical deformation of nickel foils for nanoimprint lithography on double-curved surfaces

M. R. Sonne[1*], J. Cech[2], J. H. Hattel[1] and R. Taboryski[2]

[1]Technical University of Denmark, Department of Mechanical Engineering
[2]Technical University of Denmark, Department of Micro- and Nanotechnology
*email corresponding author: mrso@mek.dtu.dk

ABSTRACT

In the present work, a manufacturing process for transferring nano-structures from a glass wafer, to a double-curved insert for injection moulding is demonstrated. A nano-structure consisting of sinusoidal cross-gratings with a period of 426 nm is successfully transferred to hemispheres on an aluminium substrate with three different radii; 500 µm, 1000 µm and 2000 µm, respectively. The nano imprint is performed using a 50 µm thick nickel foil, manufactured using electroforming. During the imprinting process, the nickel foil is stretched due to the curved surface of the aluminium substrate. Experimentally, it is possible to address this stretch by counting the periods of the cross-gratings via SEM characterization. A model for the deformation of the nickel foil during nanoimprint is developed, utilizing non-linear material and geometrical behaviour. Good agreement between measured and numerically calculated stretch ratios on the surface of the deformed nickel foil is found, and it is shown, that from the model it is also possible to predict the geometrical extend of the nano-structured area on the curved surfaces.

KEYWORDS: Nanoimprint lithography, double-curved surface, injection moulding, nickel foil, finite element model, deformation modelling.

1. INTRODUCTION

Functional nanostructures on double-curved surfaces have attracted increasing attention in the industry. Examples of functional nanostructures are well known from nature, where organisms and plants possess optical, adhesive, and self-cleaning capabilities [1]. The scientific literature is rich in examples of advanced materials emulating the well-known super-hydrophobic effect of the lotus leaf [2] and adhesive surfaces of the gecko's feet [3]. Structural colors and iridescence are most often observed in invertebrates such as butterflies and beetles, but also in the feathers of birds [4,5]. Structural color and iridescence may originate from two fundamentally different structures, 1) interference from multiple layers with different index of refraction, or 2) photonic crystals [6] where light is scattered from regularly spaced nanostructures (e.g. pillars or ridges) on the surface. The work presented in this paper is a part

of a larger project called NANOPLAST. The aim of this project is to produce injection moulding tool inserts with nano-patterned functional surfaces as mentioned above. In order to manufacture these structures on the double-curved surfaces of the injection moulding tool inserts, a technology called nanoimprint lithography (NIL) with flexible stamps is an opportunity. In literature, imprinting on simple curved surfaces using flexible materials has recently been demonstrated. Bender et al. (2006) [10] investigated the resolution, dimension stability and reproducibility of the Soft UV-Nanoimprint technique. Y-P Chen et al. did in 2008 [8] present their work on fabrication of concave gratings by curved surface UV-nanoimprint lithography, where a preshaped film was used to provide a uniform pressure distribution throughout the whole concave substrate. Ji et al. (2010) [9] used UV-SCIL (substrate conformal imprint lithography), with a flexible PDMS stamp in their work on photonic crystals patterning in LED manufacturing. In all these cases, the resolution limit due to distortion of the stamp when the pressure was applied, and complications regarding deformations of the flexible stamp, were addressed as major concerns when dealing with flexible stamps on not planar surfaces. Bending and stretching of the flexible stamp is also the main problem when doing imprint on the curved injection moulding tool inserts. As the nanostructures are created on the flexible stamp in its 2-D planar shape, these structures are deformed when the stamp is stretched. In order to take the stretching and deformations of the stamp into account when the stamp is designed, prediction of the 3-D shape is essential. This can be done by numerical simulations. Within the field of nanoimprint lithography, there is however a lack of modelling and simulating the deformation process of the flexible stamp on curved surfaces. First recently, Sonne and Hattel [11] presented a model for the constitutive and frictional behaviour of PTFE flexible stamps for nanoimprint lithography.

A nickel foil is often used as the imprinting flexible stamp. The reason for that is the way it is manufactured by electroplating, where the nickel is grown on a silicon wafer with the desired nano-structures on its surface. The nano-structures on the nickel foil are then transferred to the curved surface of the actual substrate via embossing into a polymer resist. The aim of this paper is to address the mechanical deformations of the nickel foil during this nanoimprinting manufacturing process. A series of experiments is performed, where nickel foil is used to make nanoimprint of a predefined nanopattern consisting of a sinusoidal cross-grating with a period of 426 nm, on curved aluminium inserts consisting of hemispheres with different radii. A finite element model is developed for simulating the imprinting process, predicting the distortions and strains acting in the nickel foil during manufacturing. From the deformation of the cross-grating during imprinting, the stretch of the foil is measured and compared with the results obtained from the numerical model.

2. THE MANUFACTURING PROCESS

The route from deciding a specific nano-structured surface to having the final tool insert for the injection moulding machine is long and complicated, and includes many different engineering disciplines. In Fig. 1, the manufacturing process used in this work, is schematically shown. First a glass wafer is coated with a thin layer of photoresist (A). On the backside of the glass wafer, an absorber to catch light is deposited (B), and the photoresist is then exposed with two interfering light sources (C), which create a perfectly regular cross-grating with a predefined period. The photoresist is then developed, leaving the desired nano-structure on the glass wafer (D). A thin layer of chromium is then deposited on this surface (E) in order to make it conductive, so that the nickel foil via electroplating can be formed (F). The insert tool is planarized with a resist called Hydrogen Silsesquioxane (HSQ), which when cured becomes a hard, durable and tough film, ideal for injection moulds. The nickel foil is then by a huge pressure up to 800 bar pressed into the HSQ (H), making the imprint with the

nano-structures. The HSQ on the mould insert is then finally cured, ready to be used for injection moulding of polymer parts (I).
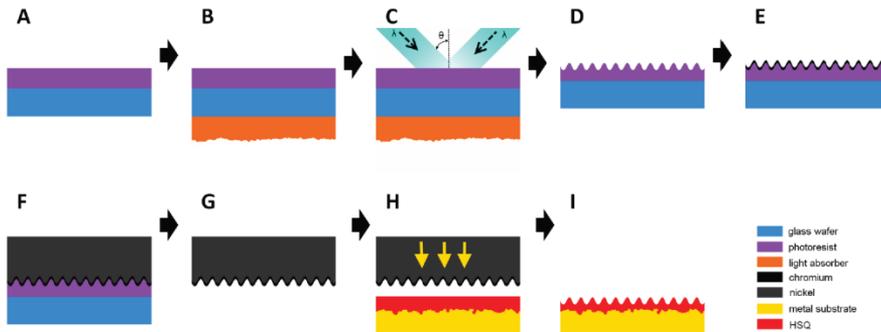

Fig.1: Schematic illustration of the manufacturing process, from preparation of the 426 nm pattern on the wafer (A-D), to electroforming the flexible nickel foil (E-G), further on to nanoimprint lithography into a material called HSQ on top of the final metal substrate (H-I).

3. APPLICATION

The manufacturing process is now applied on three aluminum inserts, which on the surface have a concave part of a hemisphere with varying radius; 500 µm, 1000 µm and 2000 µm, but with a constant height of 200 µm, see Fig. 2. These inserts are designed with the purpose of investigating, how the nickel foil behaves, when it is applied on curved surfaces with a very small radius of curvature. The deformation of the nickel foil is investigated both experimentally and numerically.
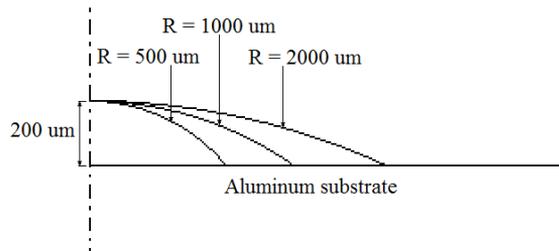

Fig. 2: Aluminum inserts with concave parts of a hemispheres with three different radii, but a constant height.

3.1. Experiment

As mentioned, the tested nanopattern is a sinusoidal cross-grating, formed by two exposures using a laser interference method on a 1.5 µm thick layer of photoresist, spin-coated on a 100 mm glass wafer. A polymer backside absorber was used to prevent back reflections of the laser beams into the photoresist. The exposed resists are developed, and the recorded amplitude grating pattern is converted to the surface corrugated phase grating, which is then electroplated with nickel, after coating with the a 60 nm chromium seed layer. The desired thickness of the electroformed nickel foil depends on the accumulated charge in the electroplating process. For this experiment, films of thickness 55±4 µm are used. The

nanopattern period on the nickel foil is was measured with an Atomic Force Microscope (AFM) to be 426.2±0.5 nm. Aluminum alloy 6061 was used as material for the tool inserts. The HSQ resist is then spray-coated on to the aluminium surface with an ultrasonic nozzle. Spray coated films consists of hard, almost solvent-free particles and have to be re-saturated with solvent prior to full cross-linking in order to ensure that the resist will flow during the nano imprint. The nano imprint is performed using a special fabricated tool, that via a piston, creates a pressure, which presses the nickel foil into the HSQ surface on the aluminium insert tools, see Fig. 3.

Fig. 3: The device for high pressure nanoimprinting of the nickel foil into the aluminium curved surface. The piston in the top of the device is pressed down in a hydraulic press.

After imprint (60 s at 650 bar) the HSQ film is thermally cured at 400 °C for 1 hour to ensure that the resist is fully cured, as reported previously in literature [12]. A Scanning Electron Microscope (SEM) (FEI Nova NanoSEM 600), operated at low vacuum mode is used to characterize the nano imprinted surfaces. Using top-view and SEM stage movement, the X and Y periods of the replicated nanopattern are measured on the spherical surfaces, in the alternating positions, while increasing the radial off-center distance. The X and Y periods are then used to calculate the mean period for each of the investigated radial positions. Note that geometrical correction needs to be applied to compensate for the increasingly curved position. The real observed period Λ_{REAL} is then calculated using this correction. This is presented later in Fig. 9.

$$\Lambda_{REAL} = \frac{\Lambda_{MEASURED}}{\cos(\vartheta)} = \frac{\Lambda_{MEASURED}}{\sqrt{1-\left(\frac{l}{R}\right)^2}} \tag{1}$$

, where ϑ is

$$\vartheta = \arcsin\left(\frac{l}{R}\right) \tag{2}$$

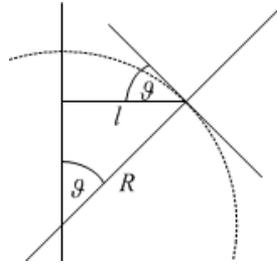and the l and R are distances on a spherical surface, according to Fig. 4.

Fig. 4: Sketch showing the relation between radius of curvature, *R*, the distance from the center to the measuring point, *l*, and the tilt angle at this point, ϑ.

3.2. Numerical model

In order to support the experimentally obtained results and to get a better understanding of the mechanical development taking place during the imprinting process, deformation of the nickel foils used for the three cases with double-curved surfaces in terms of spheres with radii of 2000 µm, 1000 µm and 500 µm, respectively, are modeled through numerical simulations via finite element analysis (FEA). Modeling this deformation is not trivial, as many different non-linearities have to be taken into account in order to get proper results; Large deformations makes the geometrical calculations non-linear, the material acts elasto-plastic, and finally, contact between substrate and nickel foil adds another non-linearity to the system of equations, which also has to be addressed.

The nickel foil is fabricated via electroplating, where the glass wafer in a nickel bath solution works as cathode and by means of a voltage potential nickel is deposited onto the wafer. What influence this deposition of nickel has on its mechanical properties is not investigated in this study, instead the mechanical behavior of nickel was found in literature [13]. Nickel has elastic properties in terms of Young's modulus $E = 200$ GPa, and a Poisson's ratio $v = 0.31$. The overall mechanical behaviour in terms of the stress related to the total strain is shown in Fig. 5.
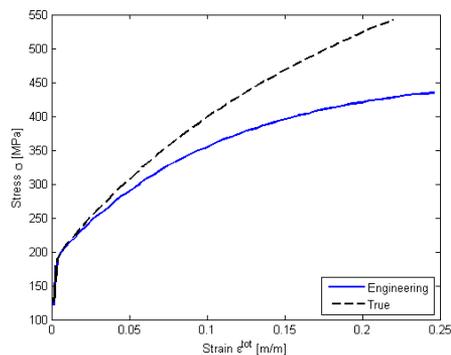

Fig. 5: Stress-strain curve of nickel given in both engineering and true values [13]

From this figure it is seen that the material shifts to deform plastically at a yield stress around 200 MPa. For calculation of the displacements, strains and stresses, a standard mechanical model based on the solution of the three static force equilibrium equations is used, i.e.

$$\sigma_{ij,i} + p_j = 0 \tag{3}$$

for $i,j = 1..3$, where p_j is the body force at any point within the nickel foil and σ_{ij} is the stress tensor. Hooke's law and linear decomposition of the strain tensor as well as large strain theory, taking the large deformations into account, are applied. The equivalent plastic strain is calculated on basis of standard J_2 flow theory, with a von Mises yield surface, where the material starts yielding when the equivalent stress (σ_e) reaches the yield stress (σ_y). The equivalent plastic strain increment couples to the deviatoric stress tensor through von Mises yield surface and the associated flow rule. Contact between substrate and nickel foil is in this case modeled via standard Coulomb friction, governed by the equation

$$F_f \leq \mu F_n \tag{4}$$

, where F_f is the force of friction exerted by each surface on the other. It is parallel to the surface, in a direction opposite to the net applied force. μ is the coefficient of friction, which is an empirical property of the contacting materials. F_n is the normal force exerted by each surface on the other, directed perpendicular (normal) to the surface. The Coulomb friction F_f may take any value from zero up to μF_n, and the direction of the frictional force against a surface is opposite to the motion that surface would experience in the absence of friction. For the contact between the aluminum substrate and the nickel foil, the friction coefficients was found in literature to be $\mu = 0.35$ [14]. The layer of HSQ is in this case not taken into account, as it was not possible in literature to find experimental data of its frictional behavior.

The system of equations mentioned in the previous section (eq. (3)) is numerically discretized through a finite element formulation and solved using the general purpose finite element code ABAQUS. In this case a 2-D axisymmetric model is used, where only aluminum substrate and nickel foil is taken into account, see Fig. 6.
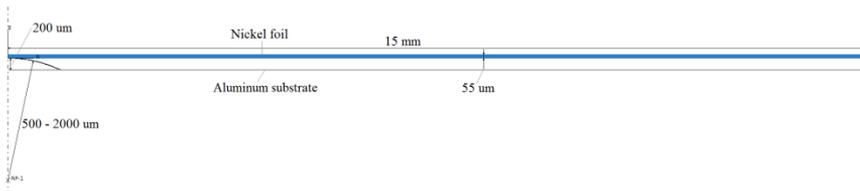

Fig. 6: Geometry in the numerical model.

On top of the nickel foil a pressure is applied, which should end up having a value of 650 bar after 60 seconds. However, this cannot instantaneously be applied in the model as this will result in a diverging solution. Instead the pressure needs to be increased gradually, so static equilibrium in subsequent increments has time to adjust.

4. RESULTS

From the experiments, it is from SEM and AFM now possible to characterize the nano imprinted 426 nm sinusoidal cross-grating on the surface of the aluminium tool inserts, see Fig. 7. It is seen that the nano-structures are very well replicated onto the metal surface. From the SEM the period of the nano-structures can now be measured, and comparison with the numerical model can be carried out.
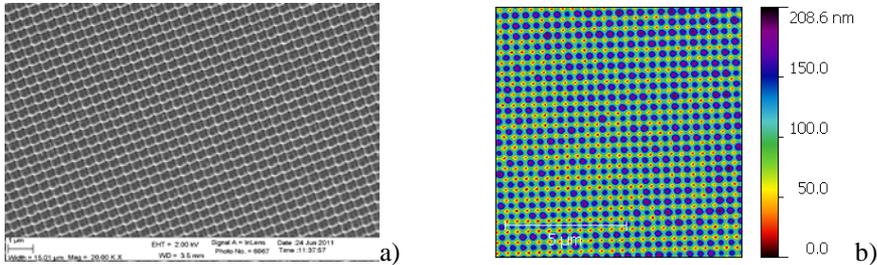

a)

b)

Fig. 7: Characterization of the nano-structured surface of the aluminium tool inserts with a) SEM and b) AFM, on the $r = 2000$ µm curved surface.

From the results of the numerical calculations, it is first of all possible to see the deformed shape of the nickel foil, when it is subjected to 650 bar. In Fig. 8, the deformed shape of the nickel foils in the three different cases is shown with a contour plot of the maximum principal logarithmic strain.
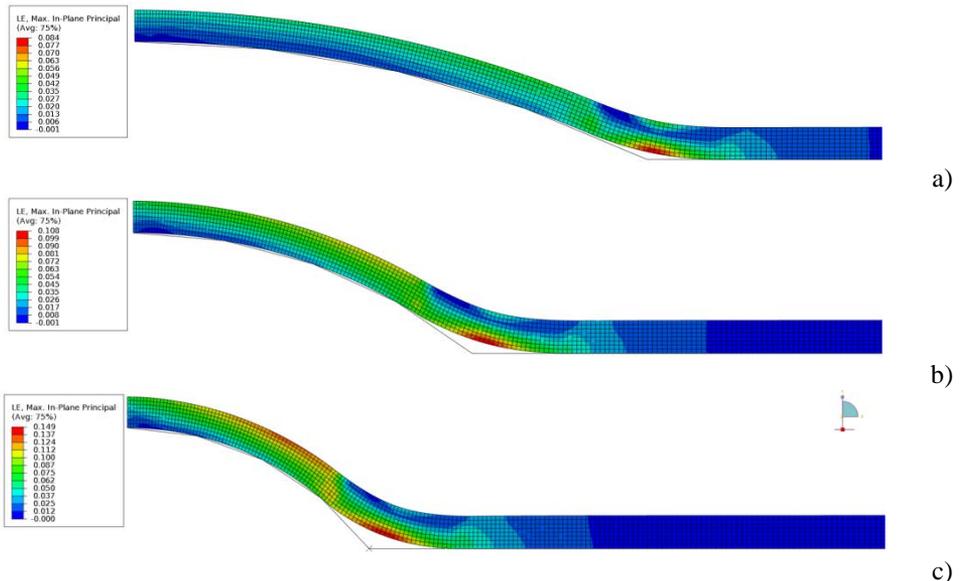

a)

b)

c)

Fig. 8: Contourplots of the deformed shapes of the nickel foils pressed down to the aluminum substrate in the three different test cases: a) curvature = 2000 µm, b) curvature = 1000 µm and c) curvature = 500 µm.

In order to compare the simulation results with the experiments, the maximum principal logarithmic strain is extracted from the model through a path on the surface on the nickel foil. With a base period of the nanostructure of 426 nm, it is possible to calculate the period on the stretched nickel foil by using equation (1). In Fig. 9, a comparison between numerical and experimental results of the grid period is shown. It is seen that the results from the simulations well matches the measured values of periods from the experiments, after they have been geometrically corrected as explained in section 3. The experimental results only show the stretching of the nickel foil, where it was possible to measure the periods of the nanostructures, whereas the results from the FE model further shows the "stretch history" all the way down the spherical cap.

From the simulations it is also possible to back out the contact pressure between the nickel foil and the aluminum substrate, see Fig 10. From this figure it is discovered that the contact pressure in the region of the spherical cap is much higher than the applied 650 bar. Moving away from the center, the pressure increases to a peak value and then rapidly descreases to zero. This is where the nickel foil stops touching the aluminum substrate, which in the numerical model results in some pressure singularities. This point is also possible to observe in the experiments, where the nanopatterns on the aluminum insert is no longer replicated from the nickel foil. It is seen, that there is a good agreement between the model and the experiments in where this waste region is placed on the aluminum substrate, which furthermore verifies the setup of the numerical model, and that it with the model also is possible to predict the limitations of making nano imprints on double-curved surfaces, applying the suggested manufacturing technology.

5. CONCLUSION

In the present work, a manufacturing process for transferring nano-structures from a glass wafer to a double-curved aluminium insert for plastic injection moulding has been demonstrated. A nano-structure consisting of sinusoidal cross-gratings with a period of 426 nm was successfully transferred to hemispheres with three different radii, 500 µm, 1000 µm and 2000 µm, respectively. The nano imprint was performed using a 50 µm thick nickel foil, manufactured with electroforming into a glass-like resist called HSQ, with a huge pressure of 650 bar over 60 seconds. During the imprinting process the nickel foil was stretched due to the curved surface of the aluminium substrate and it was experimentally possible to address this stretch by counting the periods of the cross-gratings via SEM characterization. A numerical model for simulating the deformation of the nickel foil during nano imprint was also developed, utilizing non-linear material and geometrically behaviour. Good agreement between measured and numerically calculated stretch ratios on the surface of the deformed nickel foil was found, and from the model it was also possible to predict the limits of the nano-structures on the curved surfaces, with decreasing radii.
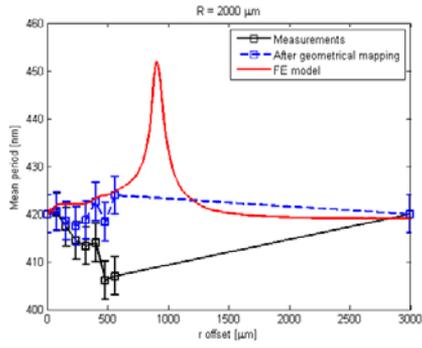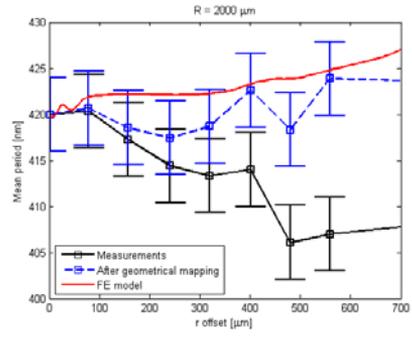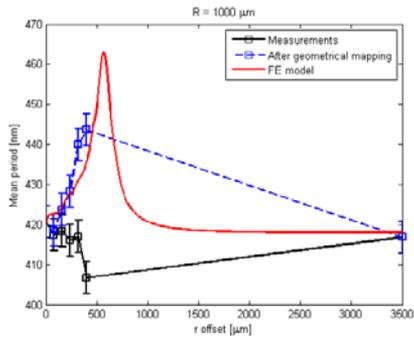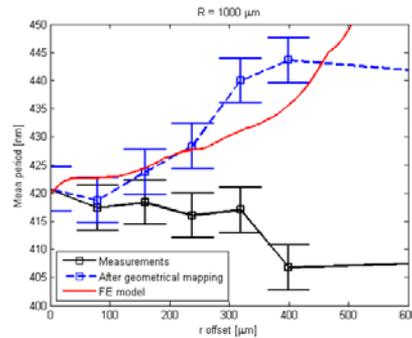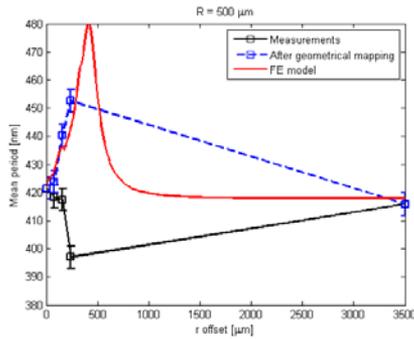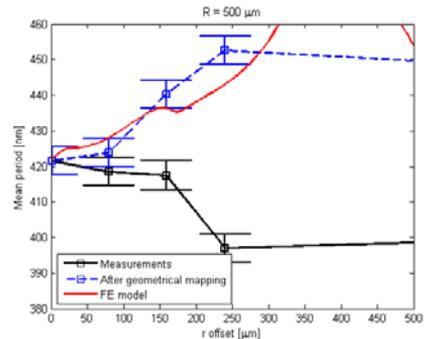
Fig. 9: Comparison of measured and numerically calculated periods of the nanostructure in the three different test cases: a) + b) 2000 µm, c) + d) 1000 µm and e) + f) 500 µm.
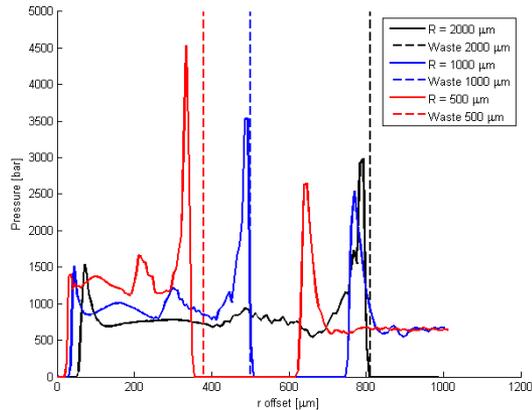
Fig. 10: Contact pressure between aluminum and nickel foil as a function of the distance along the spherical cap. The waste region (place where the nanopattern vanishes in the measurements from the experiments) is also plotted for comparison.

ACKNOWLEDGEMENTS

REFERENCES

[1] Pokroy B, Epstein A K, Persson-Gulda M C M, Aizenberg J, Adv. Mater. 2009, 21, 463–469

[2] Barthlott W, Neinhuis C, Planta 1997, 202, 1

[3] Ruibal R, Ernst V, Morphol J. 1965, 117, 271

[4] Parker A.R, J. Opt. A 2000, 2, R15–R28.

[5] Kinoshita S,Yoshioka S, and Miyazaki J, Rep. Prog. Phys. 2008, 71, 076401

[6] Matejkova-Plskova J, Shiojiri S, Shiojiri M, J. Microsc. 2009, 236, 88–93

[7] S. Nazum, MEng. Thesis, Univ. Southampton, 2007

[8] Y-P Chen et al., J. Vac. Sci. Technol. B, 2008, p. 1690

[9] Ji et al., Microelectronic Engineering, 2010, p.963

[10] M. Bender, U. Plachetka, R. Ji, A. Fuchs, B. Vratzov, H. Kurz, T. Glisner, F. Lindner, J. Vac. Sci. Tech. B 22(6) (2004) 3229–3232.

[11] M. R. Sonne, J. H. Hattel , Microelectronic Engineering, 2013 , volume 106 , pp. 1-8

[12] J. Cech, H. Pranov, G. Kofod, M. Matschuk, S. Murthy, R. Taboryski, , Appl. Surf. Sci. 2013(0).

[13] Atlas of Stress-Strain Curves, 2nd Ed., ASM International, 2002, 816 pages

[14] D. H. Buckley and R. L. Johnson, Friction and wear of Nickel-Aluminum alloys and some sulfur-modified steels in vacuum to 10e-9 millimeter of mercury, NASA Technical note, May 1964